The Company of
Biologists

RESEARCH ARTICLE

Conspecific aggregations mitigate the effects of ocean acidification on calcification of the coral *Pocillopora verrucosa*

Nicolas R. Evensen[1,2,*] and Peter J. Edmunds[1]

ABSTRACT

In densely populated communities, such as coral reefs, organisms can modify the physical and chemical environment for neighbouring individuals. We tested the hypothesis that colony density (12 colonies each placed ~0.5 cm apart versus ~8 cm apart) can modulate the physiological response (measured through rates of calcification, photosynthesis and respiration in the light and dark) of the coral *Pocillopora verrucosa* to partial pressure of CO_2 (P_{CO_2}) treatments (~400 μatm and ~1200 μatm) by altering the seawater flow regimes experienced by colonies placed in aggregations within a flume at a single flow speed. While light calcification decreased 20% under elevated versus ambient P_{CO_2} for colonies in low-density aggregations, light calcification of high-density aggregations increased 23% at elevated versus ambient P_{CO_2}. As a result, densely aggregated corals maintained calcification rates over 24 h that were comparable to those maintained under ambient P_{CO_2}, despite a 45% decrease in dark calcification at elevated versus ambient P_{CO_2}. Additionally, densely aggregated corals experienced reduced flow speeds and higher seawater retention times between colonies owing to the formation of eddies. These results support recent indications that neighbouring organisms, such as the conspecific coral colonies in the present example, can create small-scale refugia from the negative effects of ocean acidification.

KEY WORDS: High P_{CO_2}, Coral growth, Facilitation, Species interactions, Hydrodynamics

INTRODUCTION

In diverse and densely populated communities, such as coral reefs and rainforests, sessile organisms can experience different physical conditions depending on the type, size and proximity of neighbouring organisms (Helmuth et al., 1997; Henry and Aarssen, 1999; Cornell and Karlson, 2000; Callaway, 2007). Upstream coral colonies, for example, can modify the seawater flow regimes experienced by downstream colonies (Sebens et al., 1997; Hench and Rosman, 2013), and closely spaced trees in temperate forests can modify the nitrogen and carbon content of the soil in which they grow (Finzi et al., 1998). Thus, a wide variety of species interactions become common under crowded conditions (Jones et al., 1997), with some of the best known involving competition for space (Dayton, 1971) and food (Buss, 1979). However, interactions

under crowded conditions can also be beneficial for the organisms involved (Stachowicz, 2001), and under these circumstances they can positively affect community structure through the ecological process described as facilitation (sensu Bruno et al., 2003).

Facilitation is important in multiple ecosystems (Bruno et al., 2003), including tropical coral reefs (Idjadi and Edmunds, 2006), where this type of ecological interaction can play an important role among scleractinian corals under crowded conditions (Kayal et al., 2011). Indeed, the facilitative roles of scleractinians are so strong that members of this taxon are referred to as ecosystem engineers (Jones et al., 1997) because of their roles in creating three-dimensional, wave-resistant structures that promote reef diversity through the provision of habitat and ecological niches (Bellwood and Hughes, 2001; Bruno and Bertness, 2001). At high population densities, scleractinian colonies frequently encounter one another through contact, and thereafter compete for space (Lang and Chornesky, 1990). The outcomes of this type of resource competition have largely been studied from the perspective of the negative fitness implications for the individuals involved (reviewed in Chadwick and Morrow, 2011). More recently, however, attention has focused on the possibility that coral–coral interactions can result in facilitation (rather than competition), thereby generating positive fitness consequences for interacting colonies (Bruno et al., 2003). Among scleractinians, facilitation can be found among dense, multi-specific aggregates of colonies, because, for example, such aggregations can create a physical refuge against corallivory by the seastar *Acanthaster planci* (Kayal et al., 2011), and strengthen the capacity of conspecifics to compete for space with stronger competitors (Idjadi and Karlson, 2007).

Coral colonies can also mediate the performance of neighbouring corals through modification of ambient seawater flow (Helmuth et al., 1997). The position of a coral relative to its neighbours on a centimetre-to-metre scale can alter the seawater flow speed and turbulence to which it is exposed (Hench and Rosman, 2013), thereby modifying the flux of metabolites between coral tissue and seawater (Helmuth et al., 1997; Reidenbach et al., 2006). When metabolism is mass transfer limited (sensu Thomas and Atkinson, 1997), flow-mediated metabolite flux can determine the rates of physiological functions, including the aerobic respiration of the holobiont (Bruno and Edmunds, 1998), photosynthesis of the endosymbiotic *Symbiodinium* (Lesser et al., 1994) and calcification (Dennison and Barnes, 1988). Corals exposed to reduced seawater flow speeds typically experience reduced rates of important physiological processes that rely on diffusive flux with surrounding seawater under present-day conditions of seawater carbonate chemistry (Atkinson and Bilger, 1992), and these changes generally have negative implications for fitness (Thomas and Atkinson, 1997). Under future predicted partial pressure of CO_2 (P_{CO_2}) conditions (i.e. ocean acidification; OA), at least some of the inhibitory consequences of low flow speeds for the metabolism of reef corals could be reversed, particularly for

[1]Department of Biology, California State University, 18111 Nordhoff Street, Northridge, CA 91330-8303, USA. [2]Marine Spatial Ecology Lab, Australian Research Council Centre of Excellence for Coral Reef Studies and School of Biological Sciences, The University of Queensland, St Lucia, Queensland 4072, Australia.

*Author for correspondence (nicolas.r.evensen@gmail.com)

N.R.E., 0000-0003-3318-5593

List of symbols and abbreviations

AIC	Akaike's information criterion
A_T	total alkalinity
CCA	crustose coralline algae
DBL	diffusive boundary layer
OA	ocean acidification
P_{CO_2}	partial pressure of CO_2
T_u	turbulence intensity
$\bar{U}$	mean flow speed
U_{rms}	root mean square of the turbulent velocity fluctuations
Ω_{arag}	aragonite saturation state

calcification (Chan et al., 2016). This outcome is hypothesized to occur because slow seawater flow results in thickening of the diffusive boundary layer (DBL), which favours an increased pH in the seawater above the coral tissue as a result of CO_2 uptake by photosynthesis (Chan et al., 2016), with the potentially important outcome of reducing the overall sensitivity of calcification to OA (McCulloch et al., 2012). This hypothesis is consistent with laboratory experiments in which *Favites* sp. colonies (hemispherical morphology) were incubated in flumes under low unidirectional flow speeds (0–5 cm s^{-1}), with the result that seawater pH adjacent to the tissue (and within the DBL) increased by up to 0.8 units compared with bulk seawater under reduced seawater pH of 7.8 (Chan et al., 2016).

Here we extend our analyses of the effects of OA and coral–coral interactions on coral growth (Evensen et al., 2015; Evensen and Edmunds, 2016) by testing the hypothesis that colony density affects the physiology of *Pocillopora verrucosa* (Ellis and Solander 1786) under OA conditions. Treatment effects were evaluated from the summed physiological performance of multiple colonies placed in discrete spatial arrangements within a flume (after Vogel and LaBarbera, 1978) held at a constant flow speed. The flume was sealed and operated in a closed circuit mode to measure physiological rates through the flux of diagnostic metabolites. The outcome of the experiment was assessed using response variables that characterized three aspects of the physiology of reef building corals: calcification measured the implication for holobiont growth; photosynthesis measured the response of the *Symbiodinium* symbionts and their ability to supply photosynthetically fixed carbon to the animal host (sensu Muscatine et al., 1984); and aerobic respiration measured metabolic costs under treatment conditions (Patterson et al., 1991). Dependent variables were measured in the light and dark as they are depressed in darkness in symbiotic corals (Chalker and Taylor, 1978), and it is reasonable to expect differential responses to OA and colony density relative to when they are likely to be rate-limited (i.e. during the day).

MATERIALS AND METHODS
Experimental overview
The study was conducted in April 2015 in Moorea, French Polynesia, using colonies of *Pocillopora verrucosa* (~4 cm in planar diameter) collected from the outer reef of the north shore at 10–12 m depth. The study focused on *P. verrucosa* because it is ubiquitous and ecologically important on shallow reefs throughout the Indo-Pacific (Veron, 2000), including on the outer reefs of Moorea (Bramanti and Edmunds, 2016; Edmunds et al., 2016). Corals were collected from multiple sites separated by 100–200 m on the outer reef to maximize the likelihood that the selected coral colonies were genetically unique, and transferred directly to an acclimation tank (described below).

The experiment used a sequential design, in which corals first were incubated under ambient or elevated P_{CO_2} in flow-through tanks, and then were incubated in a recirculating flume under the same P_{CO_2} crossed with a contrast of two colony densities (Fig. S1). Two response variables were measured in the light (calcification and net photosynthesis at a single irradiance), two response variables were measured in the dark (aerobic respiration and calcification) and two response variables were calculated from these values (gross photosynthesis, and calcification integrated over 24 h). Aerobic respiration was measured as oxygen uptake, and net photosynthesis was measured as the flux of oxygen at a constant irradiance. Oxygen uptake (respiration) was thus given a negative notation and oxygen evolution (net photosynthesis) a positive notation, with gross photosynthesis obtained by subtracting respiration from net photosynthesis. Daily calcification was calculated by integrating calcification in the light over 12 h, calcification in the dark over 12 h, and summing the two values assuming each day consisted of 12 h of light at a constant intensity. The six response variables were measured for aggregates of a fixed number (*n*=12) of similar-sized colonies placed in the flume in either high- or low-density arrays. With this design, it was not possible to measure the physiology of individual colonies in each aggregate, and therefore our results describe the performance corals averaged across each aggregate.

In the first phase of the experiment, corals were maintained in tanks at ambient or elevated P_{CO_2} (with three tanks in each treatment) for 8 days to allow them to acclimate to treatment conditions. Sample sizes were determined based on effect sizes in a previous experiment (Evensen and Edmunds, 2016). Colony densities were not regulated in these tanks, and the location of the colonies in the tanks was randomized daily to avoid position effects. With 12 colonies in each 60×50 cm tank, colonies typically were ~8 cm apart. The contrast of two colony densities was created in the flume to which corals periodically were staged and tested for their response to two P_{CO_2} regimes.

In the second phase of the experiment, groups of 12 colonies were selected by tank (with all corals used from any one tank) for placement in the flume at a constant flow speed at one of two densities that were crossed with one of two P_{CO_2} treatments (Fig. S1), with the order of the tanks selected at random. Each incubation lasted 2 h. The 12 corals from a single tank were placed in the 100×10 cm working section of the flume at either low density (12 colonies in an area of 90×10 cm, corresponding to 133 colonies m^{-2}) with branch tips ~8 cm apart, or high density (12 colonies in an area of 30×10 cm, corresponding to 400 colonies m^{-2}) with branch tips ~0.5 cm apart. The density and P_{CO_2} treatments were implemented in a random sequence, while light treatments took place during the day and dark treatments at night, with at least 2 h between any light and dark treatments to minimize the chance of any residual effect of light on dark metabolic activity.

Incubations were completed after sealing the flume and operating it in a closed-circuit mode, during which change in O_2 concentration and total alkalinity in the seawater were used to measure aggregate respiration, photosynthesis and calcification as described below. Following incubations, the coral colonies were returned to their respective tanks until their surface area was measured at the end of experiment (described below). This sequence of measurements required 6 days to process all six groups of 12 corals under the aforementioned conditions, and while this meant that the exposure to the first phase conditions varied from 8 to 14 days, this effect was distributed randomly among treatments.

Tank treatments

Coral colonies were collected from the reef and transferred to a 1000-litre acclimation tank (Aqualogic Inc., San Diego, CA, USA) for 1 week prior to the start of the experiment. Corals were placed upright in the acclimation tank without being attached to a plastic base, and were kept at ~700 µmol photons m^{-2} s^{-1} and 26.5°C on a submerged table that rotated at 2 revolutions day^{-1} to provide uniform exposure to physical conditions. These conditions were similar to the conditions recorded on the reef where the corals were collected, and also to those in the six treatment tanks and flume. The maximum light intensity matched the greatest light intensity experienced by the corals at ~10 m depth on the fore reef, where the corals were collected (~645 µmol photons m^{-2} s^{-1} recorded at ~12:00 h on 10 April 2007; P.J.E., unpublished data). Seawater temperature was close to the lowest temperatures experience by corals on the fore reef of Moorea (Washburn, 2016), where the mean monthly seawater temperature at 10 m depth ranged from 26.4 to 29.1°C in 2015 (Washburn, 2016). Although the ambient seawater temperature when the experiment was conducted was 28.9°C, a lower temperature was used in the experiment to reduce the likelihood of stress (e.g. bleaching) related to high temperature.

After 7 days in the acclimation tank, corals were randomly transferred to the treatments tanks, with 12 colonies placed in each of six tanks (150 litres each), three of which were maintained at ambient P_{CO_2} (~400 µatm) and three at high P_{CO_2} (~1100 µatm). The high P_{CO_2} treatment simulated elevated P_{CO_2} conditions expected by the end of the current century in a pessimistic scenario of anthropogenic gas emissions (RCP 8.5; Moss et al., 2010). The tanks received a constant supply (~400 ml min^{-1}) of seawater pumped from 12 m depth in Cook's Bay and filtered through sand with a cut-off pore size of ~100 µm. The high P_{CO_2} treatment was created by independently bubbling pure CO_2 into each of the three tanks allocated to this treatment, with the flow of CO_2 into the tanks regulated using individual pH controllers (Apex Aquacontroller, Neptune Systems, Morgan Hill, CA, USA). Ambient air was also bubbled into all six tanks to oxygenate the water.

The treatment tanks were individually illuminated with a 75 W light emitting diode (LED) module (Sol White LED Module, Aqua-Illumination, 6500 K) that produced a diel photoperiod, with light intensity rising gradually for 4 h from 06:00 h, stabilizing for 4 h at maximum intensity (700 µmol photons m^{-2} s^{-1}), and then declining for the last 4 h of the 12 h light cycle. Light was measured daily at the same depth in the tanks where the corals were placed, and measurements were made using a 4-π sensor (LI-COR LI-193SA, LI-COR, Lincoln, NE, USA) attached to a meter (LI-COR Li-1400).

Seawater temperature, pH, total alkalinity (A_T) and salinity were monitored in the treatment tanks throughout the experiment, and the values were used to calculate seawater carbonate chemistry using CO2SYS (Lewis and Wallace, 1998), with the constants of Mehrbach et al. (1973). Temperature was measured twice daily (~08:00 and 18:00 h) in each tank using a certified digital thermometer (model 15-077-8, ±0.01°C, Thermo Fisher

Scientific, Waltham, MA, USA). Seawater samples (~500 ml) were collected daily from each tank at ~08:00 h, and equilibrated to the laboratory temperature (~25°C) before processing. Seawater samples were processed within 2 h of collection for pH (daily at first, and then every other day once conditions in the tanks stabilized), salinity (every other day) and A_T (every 2–3 days). pH of the seawater was measured spectrophotometrically using m-cresol dye (SOP 6b; Dickson et al., 2007). A_T of the seawater was measured with open-cell potentiometric titrations, using an automated titrator (model T50, Mettler-Toledo) operated with 50 g seawater samples. Precision and accuracy of the titrations was measured using certified reference materials provided by A. G. Dickson (batch #130), with titrations yielding A_T values within 10 µmol kg^{-1} of the certified value. Salinity was measured using a YSI 3100 Conductivity Meter (YSI Inc., Yellow Springs, OH, USA).

Flume treatments

The flume had a clear acrylic working section 1.0×0.1×0.1 m with an open top that could be sealed to allow a closed-circuit operation, and contained 46 litres of seawater that was temperature regulated. With the top open, each group of 12 corals from one of six tanks was transferred, in a random sequence, to the flume. Each group was transferred twice to the flume, once in the low-density arrangement, and once in the high-density arrangement (Figs S1, S2; described above), and incubated in ambient or high P_{CO_2} to match the conditions in their respective treatment tanks. Physiological responses of the aggregates (described below) to the treatment conditions were measured for all 12 colonies placed in each density treatment.

Density treatments were created by randomly placing the 12 corals in fixed slots located on one of two types of flexible plastic trays. One 30×8 cm tray was used for the high-density treatment, and two 50×8 cm trays were used for the low-density treatment. The trays fitted within the working section of the flume, and held the colonies upright in fixed spatial arrays during incubations. Light intensities, temperature and carbonate chemistry during the flume incubations were matched to those maintained in the treatment tanks. The flume was illuminated with two LED modules (Sol White LED Module, Aqua-Illumination, 6500 K), which supplied light to the working section of the flume at ~700 µmol photons m^{-2} s^{-1}. Prior to each flume incubation, the flume was filled with filtered (50 µm) seawater freshly pumped from Cook's Bay and maintained at 26.5°C. The temperature in the flume was maintained by a chiller (Delta Star, DS-4, Aqua Logic, Inc.) attached to a water jacket surrounding the seawater return circuit.

For the high P_{CO_2} treatment, pure CO_2 was bubbled into the flume until seawater pH reached ~7.70, which matched the pH in the high P_{CO_2} tanks (Table 1). This procedure added bubbles of CO_2 to the flume, but these were flushed out until no visible bubbles remained prior to sealing the flume and beginning incubations. Prior to sealing the flume, pH of the enclosed seawater was measured using a portable meter (Orion 3-stars) fitted with a DG 115-SC probe

Table 1. Parameters of the carbonate chemistry in the tanks (n=6) and during flume incubations

	Treatment	Temperature (°C)	pH_T	P_{CO_2} (µatm)	A_T (µmol kg^{-1})	Ω_{arag}
Tanks	Ambient P_{CO_2}	26.5±0.1	8.00	406±4	2283±5	3.50±0.02
	High P_{CO_2}	26.6±0.1	7.70	1118±23	2292±5	1.73±0.03
Flume	Ambient P_{CO_2}	26.6±0.1	8.03	407±1	2315±2	3.55±0.01
	High P_{CO_2}	26.6±0.1	7.65	1188±13	2323±2	1.71±0.01

Values are means±s.e.m. (n=26 for temperature, n=7 for A_T and n=15 for all other parameters). pH_T, pH on the total scale; A_T, total alkalinity; Ω_{arag}, aragonite saturation state. s.e. for pH_T was <0.01. High P_{CO_2} ~1100 µatm.

(Mettler Toledo, Switzerland) that was calibrated every 2 days using 2-amino-2-hydroxymethyl-1,3-propanediol (TRIS) buffers (SOP 6a; Dickson et al., 2007). To evaluate the accuracy of the portable pH meter, pH of the seawater was also measured spectrophotometrically using m-cresol dye on samples collected prior to sealing the flume (SOP 6b; Dickson et al., 2007); values recorded with the portable pH meter were ≤ 0.02 of the pH measured spectrophotometrically. Measurements of A_T, and the subsequent calculation of seawater carbonate chemistry for each flume incubation, were conducted using the methodology described above for seawater in the tanks.

Flow speed in the flume was set to ~7 cm s^{-1} to resemble the monthly mean flow speed of 6.89±0.01 cm s^{-1} (±s.e.m., n=76 months) recorded at 10 m depth on the outer reef of the north shore of Moorea between 2006 and 2014 using a bottom-mounted Acoustic Doppler Current Profiler (Sentinel, Teledyne RD 180 Instruments; Washburn, 2016). While the flow speed in the flume was almost identical to the mean flow speed in open water above the outer reef, the experiment was completed in a small flume in which wall effects probably influenced the seawater flow (Muschenheim et al., 1986), therefore complicating the interpretation of the ecological relevance of the flow speeds to which the corals were exposed. Flow speed was measured by photographing hydrated brine shrimp eggs placed into the flume when it was filled with seawater alone (i.e. without corals) (after Johnson and Sebens, 1993).

Physiological responses

During the flume incubations, dark respiration, net photosynthesis and calcification (in the light and dark) were measured. Calcification in the light and net photosynthesis were measured simultaneously by incubating corals at a light intensity of ~700 µmol photons m^{-2} s^{-1} and flow speed of 7 cm s^{-1} for 2 h. For the simultaneous measurements of dark calcification and dark respiration, corals were kept in the dark for at least 1 h under 7 cm s^{-1} flow, as the effects of light on coral metabolism can remain for 20–30 min after incubation in the light (Roth et al., 1982; Moya et al., 2006). Calcification was measured using the alkalinity anomaly technique (Chisholm and Gattuso, 1991), with A_T measured using duplicate seawater samples collected at the beginning and end of each of the 2 h flume incubations. The stoichiometric relation of a 2 mole reduction in A_T contributing to 1 mole of CaCO$_3$ precipitated through coral calcification was used to calculate calcification (Chisholm and Gattuso, 1991). Calcification rates were corrected for control incubations performed with the flume filled with seawater but no corals. Corrected values were normalized to the combined surface area of the 12 corals in each aggregation as determined at the conclusion of the experiment using the wax dipping technique (Stimson and Kinzie, 1991).

Net photosynthesis and dark aerobic respiration were calculated from the change in O$_2$ concentration during incubations in the light and dark (respectively). Photosynthesis and respiration were corrected using control incubations performed on flumes containing only seawater. During all incubations, O$_2$ saturation in the flume was measured using an O$_2$ sensor (FOXY-R, 1.58 mm diameter, Ocean Optics, Dunedin, FL, USA), attached to a phase fluorometer (NeoFox-GT, Ocean Optics) and a computer running software (NeoFox Viewer, Ocean Optics) to continuously record O$_2$ saturation. The sensor was calibrated with a zero solution (sodium sulphite and 0.01 mol l^{-1} sodium tetraborate) and an O$_2$ maximum created using water-saturated air in a vial at the measurement temperature. O$_2$ saturation was converted to concentration using the

solubility of O$_2$ in seawater of a known salinity and temperature (N. Ramsing and J. Gundersen at Unisense, Aarhus, Denmark). Photosynthesis and respiration were normalized to the combined tissue surface area of the 12 corals in each aggregation.

Flow characteristics

Because of the strong effects of seawater flow (i.e. speed and extent to which the flow is turbulent versus laminar) on coral physiology (Dennison and Barnes, 1988; Atkinson and Bilger, 1992; Lesser et al., 1994), which act through mass flux effects at the surface of coral tissue (Helmuth et al., 1997) and seawater mixing among coral branches (Sebens et al., 1997), separate flume incubations were used to assess the flow speed and turbulence intensity between coral colonies when placed in each of the experimental densities. One randomly selected aggregation of 12 coral colonies from each P_{CO_2} treatment was used to characterize seawater flow among colonies at 7 cm s^{-1}. Flow speed and turbulence intensity were measured using photographs (taken with a Nikon D70 fitted with a Nikon 60 mm f/2.8D AF Micro-Nikkor lens) of hydrated brine shrimp eggs (after Johnson and Sebens, 1993) released into the seawater in the flume. To quantify flow speeds and turbulence intensity, photographs of the moving brine shrimp eggs were taken upstream, downstream and between coral colonies, in both the low- and high-density aggregations. Mean flow speeds ($\bar{U}$) were measured after Johnson and Sebens (1993), and turbulence intensities (T_u; unitless) were calculated after Denny (1988). T_u was calculated by dividing the root mean square of the turbulent velocity fluctuations (U_{rms}) at a particular location over a specified period of time by the mean flow speed at the same location and over the same period ($\bar{U}$). Individual values of T_u were calculated within, upstream and downstream of each aggregation density, based on individual brine shrimp egg tracks at each location.

To assess the effects of aggregation density on mass flux to the surface of corals, plaster-of-Paris casts of a single *P. verrucosa* colony were placed in the flume in both the low- and high-density aggregations. The dissolution rate of the plaster cast under a constant flow speed (7 cm s^{-1}) was used to estimate mass flux to the surface of the corals (sensu Reidenbach et al., 2006). Multiple plaster-of-Paris casts (n=24) were made of a single ~4 cm diameter *P. verrucosa* colony collected from 10 m depth on the outer reef of Moorea, and were similar in size, shape and surface structuring to the colonies used in this study. Plaster colonies were made from plaster mixes containing a constant ratio of plaster and water, and dried to a constant weight in an air-conditioned room at 23°C. The plaster replicas captured small-scale skeletal details, including verrucae and corallites (Fig. S3), and thus were accurate replicates of live *P. verrucosa* colonies.

Twenty-four plaster corals were used in two flume incubations (each lasting 4 h), first with 12 corals arranged in a dense aggregation, and second with 12 corals arranged in a low-density aggregation, as described above. Following incubations, the plaster corals were removed from the flume and weighed after reaching a constant weight in an air-conditioned room at 23°C. Additional plaster corals were placed in a bucket filled with the same seawater as contained in the flume, and left undisturbed as controls during the dissolution trial. The proportion of plaster corals dissolving in still water was multiplied by the initial mass of the plaster corals placed in the flume to correct for dissolution in still water, providing a corrected measure of the dissolution resulting from seawater motion in the flume (after Brown and Carpenter, 2015). The final dry mass of each coral cast after the flume incubations was subtracted from the corrected initial mass and expressed as a dissolution rate (g h^{-1}).

Statistical analysis

Treatment conditions in the tanks and in the flume incubations were analyzed using a nested ANOVA, with tank or flume (respectively) a random factor nested in each P_{CO_2} treatment. The nested factor was dropped from the analyses when not significant at $P \geq 0.250$ (Quinn and Keough, 2002). Treatment conditions in the ambient P_{CO_2} tanks and ambient P_{CO_2} flume incubations, and between the high P_{CO_2} tanks and high P_{CO_2} flume incubations, were compared using t-tests in order to test for homogeneity of treatments between tanks and the flume.

The six dependent variables were analyzed as a function of P_{CO_2}, colony density and tank using univariate linear mixed-effects models, in which P_{CO_2} and density were fixed effects, and tank was a random effect (nested within P_{CO_2}). Akaike's information criterion (AIC) was used to infer the best supported model(s) of the main effects and interactions (i.e. the model with the lowest AIC). A maximal model was fitted including factors and interaction terms, and the least significant terms were removed sequentially, starting with the highest-order interactions (sensu Harborne et al., 2011). Each time a term was removed from the model, the reduced model (with the removed term) was compared with the model that included the term using a Chi-square test to ensure that the term removed did not significantly (i.e. $P<0.05$) alter the model. Terms were removed until the model contained only significant terms, or until removal of any non-significant terms resulted in a significant alteration to the model, as evaluated by the Chi-square test ($\alpha=0.05$). The final model used a restricted maximum likelihood model to analyze the effects of the significant factors on the response variables. Finally, dissolution rates of the coral casts in the low- and high-density aggregations were compared using a t-test. All analyses were performed using R software (http://www.R-project.org), using the packages lme4 (http://CRAN.R-project.org/package=lme4) and nlme (http://CRAN.R-project.org/package=nlme).

RESULTS

Tank and flume treatment conditions

The conditions in the treatment tanks were accurately regulated (Table 1), with light averaging 686 ± 4 µmol photons m^{-2} s^{-1} ($n=168$) and salinity averaging 35.5 ± 0.04 ($n=36$), pooling across all times and tanks ($\pm$s.e.m.). Temperature did not differ between treatments ($F_{1,4}=0.533$, $P=0.467$), but differed between tanks within treatments ($F_{4,152}=10.2$, $P=0.002$), though differences between tanks were ≤0.4°C. Analysis of seawater chemistry revealed that P_{CO_2}, pH and aragonite saturation state (Ω_{arag}) differed between treatments ($F_{1,4}\geq961$, $P<0.001$), but not tanks ($F_{4,86}\leq0.536$, $P\geq0.466$). A_T did not vary among tanks ($F_{4,38}=0.571$, $P=0.455$) or treatments ($F_{1,4}=1.25$, $P=0.270$).

In the flume incubations, temperature did not differ between ($F_{1,4}=0.567$, $P=0.456$) or within P_{CO_2} treatments ($F_{4,44}=0.757$, $P=0.389$). P_{CO_2}, pH and Ω_{arag} differed between P_{CO_2} treatments ($F_{1,4}\geq9818.935$, $P<0.001$), but not flume trials ($F_{4,86}\leq1.614$, $P\geq0.211$). A_T did not differ between flume trials within treatments ($F_{4,44}=2.811$, $P=0.164$), but did differ between P_{CO_2} treatments ($F_{1,4}=6.452$, $P=0.015$), with mean values differing by 8 µmol kg^{-1}.

Conditions in the flumes were regulated to resemble conditions in the tanks, with light averaging 679 ± 5 µmol photons m^{-2} s^{-1} ($n=24$), and salinity averaging 35.6 ± 0.01 (both $\pm$s.e.m., $n=24$) pooled among incubations (Table 1). Temperature did not differ between the tanks and flume under ambient and high P_{CO_2} ($t\leq0.446$, d.f.=81, $P\geq0.657$). Additionally, pH and Ω_{arag} did not differ between the ambient tanks and ambient flume incubations ($t\leq1.94$, d.f.=47, $P\geq0.057$), or between the high P_{CO_2} tanks and high P_{CO_2} flume trials ($t\geq2.08$, d.f.=47, $P>0.15$). Conversely, P_{CO_2} did not differ between the ambient tanks and ambient flume incubations ($t=0.185$, d.f.=47, $P=0.085$), but did differ between the high P_{CO_2} tanks and high P_{CO_2} flume trials ($t=2.56$, d.f.=47, $P=0.013$); mean P_{CO_2} was 5% higher in the flume compared with the tanks (Table 1). A_T differed between tanks and flumes at both ambient and high P_{CO_2} ($t\geq4.12$, d.f.=26, $P<0.001$), with mean A_T 1% higher in the flumes for both P_{CO_2} conditions (Table 1).

Physiological results

All the corals in the experiment maintained a healthy appearance, with no signs of bleaching or tissue death, and no corals were excluded from the experiment. For calcification in the light, the model that best explained the data included the interaction between P_{CO_2} and aggregate density (Table 2). Mean calcification in the light for corals in the low-density aggregations decreased by 20% from 1.11 ± 0.06 mg cm^{-2} day^{-1} under ambient P_{CO_2} to 0.89 ± 0.08 mg cm^{-2} day^{-1} ($\pm$s.e.m., $n=3$) under high P_{CO_2}. Conversely, mean calcification in the light for corals in the high-density aggregations increased by 23% from 0.87 ± 0.05 mg cm^{-2} day^{-1} under ambient P_{CO_2} to 1.07 ± 0.06 mg cm^{-2} day^{-1} (both $\pm$s.e.m., $n=3$) under high P_{CO_2} (Fig. 1). For calcification in the dark, the best model explaining the data contained only P_{CO_2} (Table 2), with mean calcification decreasing 38% from 0.40 ± 0.05 mg cm^{-2} day^{-1} under ambient P_{CO_2}, to 0.25 ± 0.06 mg cm^{-2} day^{-1} under high P_{CO_2} ($\pm$s.e.m., $n=6$, pooling low and high density aggregations). For calcification integrated over 24 h, the model that best explained the data contained neither the interaction term nor the main factors, and indicated that integrated calcification was unaffected by P_{CO_2} or density (Table 2).

Net photosynthesis and respiration were best explained by models containing neither the interaction term nor the main factors (Table 2). Mean net photosynthesis was similar between treatments, and for low-density aggregations, mean values were 0.96 ± 0.11 µmol O_2 cm^{-2} h^{-1} under ambient P_{CO_2} and 1.04 ± 0.23 µmol O_2 cm^{-2} h^{-1} under high P_{CO_2} ($\pm$s.e.m., $n=3$). For colonies in high-density aggregations, mean net photosynthesis was 0.82 ± 0.19 µmol O_2 cm^{-2} h^{-1} under ambient P_{CO_2} and $0.94\pm$

Table 2. Generalized linear mixed-effects models for the effect of P_{CO_2} and spatial arrangement on *Pocillopora verrucosa*

Model term	Response variable				
	Light calcification	Dark calcification	Integrated calcification	Net photosynthesis	Respiration
Intercept	0.867 (<0.001)	0.405 (<0.001)	0.657 (<0.001)	0.939 (<0.001)	−0.359 (<0.001)
P_{CO_2}	n.s.	−0.152 (0.118)	n.s.	n.s.	n.s.
Aggregation	n.s.	n.s.	n.s.	n.s.	n.s.
$P_{CO_2}\times$Aggregation	−0.427 (0.031)	n.s.	n.s.	n.s.	n.s.

Values are model coefficients with P-values in parentheses. Integrated calcification is the mean calcification based on light and dark calcification rates. n.s., non-significant term ($P>0.05$). A non-significant term is included in the table, as its removal resulted in a significant increase in deviance, indicating a non-significant influence of P_{CO_2} on dark calcification.
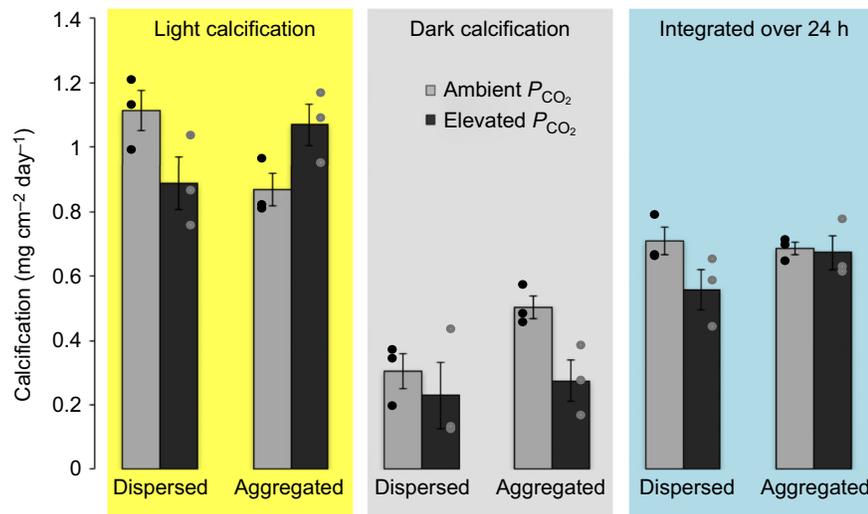
Fig. 1. Light, dark and integrated calcification of whole *Pocillopora verrucosa* colonies (~4 cm diameter) in low- and high-density aggregations (*n*=12 individuals per aggregation), and incubated in ambient P_{CO_2} (~400 µatm) or high P_{CO_2} (~1100 µatm) seawater. Bars represent means±s.e.m. (*n*=3 for all treatments), with black and grey circles representing individual replicates in each ambient and high P_{CO_2} treatment, respectively. Data were analyzed using generalized linear mixed-effects models, with a significant interaction between P_{CO_2} and aggregate density for light calcification (*P*=0.031).

0.19 µmol O_2 cm^{-2} h^{-1} under high P_{CO_2} (±s.e.m., *n*=3; Fig. 2). Similarly, respiration rates did not differ between treatments, and for low-density aggregations, mean values were 0.47±0.10 µmol O_2 cm^{-2} h^{-1} under ambient P_{CO_2} and 0.32±0.06 µmol O_2 cm^{-2} h^{-1} under high P_{CO_2} (±s.e.m., *n*=3). Finally, in high-density aggregations, mean respiration rates were 0.36±0.06 µmol O_2 cm^{-2} h^{-1} under ambient P_{CO_2} and 0.29±0.05 µmol O_2 cm^{-2} h^{-1} under high P_{CO_2} (±s.e.m., *n*=3).

Flow characteristics and mass flux
Seawater flow was laminar above and upstream of the corals in the working section of the flume (*Re*=141), with mean flow speeds ($\bar{U}$) of 6.98±0.04 cm s^{-1} (±s.e.m., *n*=36) and a turbulence intensity (T_u) of 0.04, ~1 cm above the high-density aggregate. $\bar{U}$ decreased to 0.55±0.07 cm s^{-1} within the high-density aggregations (i.e. between corals in the middle rows of the aggregation), and 0.50± 0.06 cm s^{-1} (±s.e.m., *n*=36) directly behind the last downstream row of colonies. T_u was three times higher behind the last downstream colony of the aggregation (0.12), and over four times higher (0.17) within the aggregation compared with directly above the aggregation (0.04), with eddies forming between the rows of the aggregation and behind the last downstream row of the aggregation.

Eddies also formed downstream of corals in the low-density aggregation, with $\bar{U}$ decreasing from 6.92±0.05 cm s^{-1} above the

corals to 0.75±0.07 cm s^{-1} (±s.e.m., *n*=36) behind coral colonies. Additionally, T_u values were over four times higher (0.19) downstream of corals in the low-density aggregates than above the corals. Because of the spacing between the corals, turbulence persisted downstream of the low-density aggregations (Fig. 3B), with T_u remaining at 0.19 cm s^{-1} to a distance of ~6–7 cm downstream of the colonies. However, flow speeds increased to 3.64 ±0.07 cm s^{-1} (±s.e.m., *n*=36) compared with directly behind the nearest upstream colony, when moving seawater reached the nearest downstream colony in the low-density aggregates.

Results from the analysis of the dissolution of plaster corals reflected the difference in flow speeds experienced by the colonies in each of the aggregates, with dissolution rates marginally different between colonies placed in low- versus high-density aggregations (*t*=2.07, d.f.=22, *P*=0.05). Mean dissolution rates were 22% higher in the low-density aggregation (0.62±0.04 g h^{-1}) versus the high-density aggregation (0.49±0.05 g h^{-1}; ±s.e.m., *n*=12).

DISCUSSION
The present study investigated the interactive effects of coral colony density and P_{CO_2} on coral physiology at a constant flow speed. Our results support the hypothesis that adjacent small coral colonies (i.e. ≤0.5 cm apart) can modulate the effects of ocean acidification on coral physiology. Critically, mean calcification in the light of
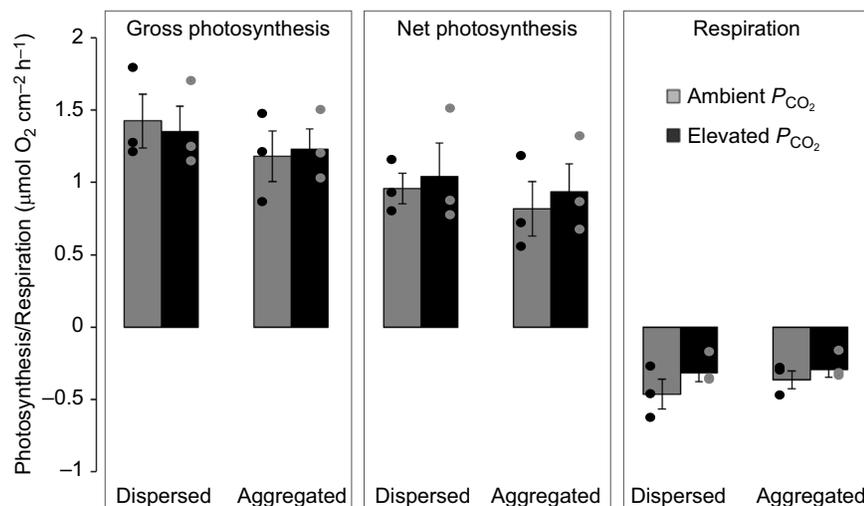

Fig. 2. Gross photosynthesis, net photosynthesis and respiration rates of whole *Pocillopora verrucosa* colonies (~4 cm diameter) in low- or high-density aggregations (*n*=12 individuals per aggregation), and incubated in ambient P_{CO_2} (~400 µatm) or high P_{CO_2} (~1100 µatm) seawater. Bars represent means±s.e.m. (*n*=3 for all treatments), with black and grey circles representing individual replicates in each ambient and high P_{CO_2} treatment, respectively. Data were analyzed using generalized linear mixed-effects models, with no significant effect of P_{CO_2} or aggregate density on any of the responses.
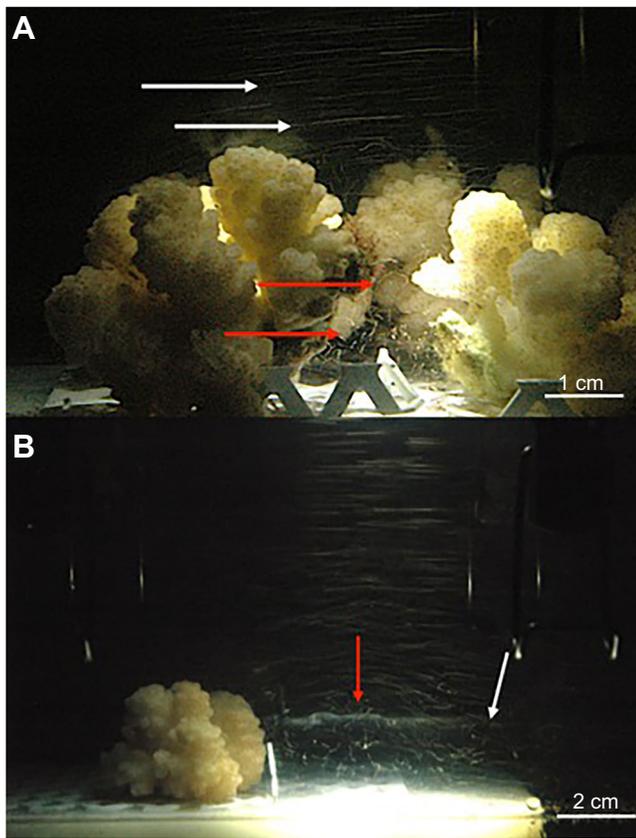
Fig. 3. Photographs of flumes containing hydrated brine shrimp eggs during trials used to quantify flow. (A) Corals in the high-density treatment with arrows indicating the direction of seawater flow. White arrows show streaks created by photographing brine shrimp eggs with a low shutter speed (0.2 s), with the streak visualizing the flow above the corals at ~7 cm s^{-1} (bulk flow speed in the flume). Red arrows show the brine shrimp eggs caught in an eddy behind the upstream coral colony. (B) A coral in the low-density treatment with the red arrow showing the eddy downstream of the coral colony, and the white arrow indicating where the turbulence created by the upstream colony starts to dissipate.

densely aggregated colonies of *P. verrucosa* increased by 23% at 1188 µatm P_{CO_2} compared with densely aggregated corals at ambient P_{CO_2}. In contrast, calcification decreased by 20% under elevated P_{CO_2} for colonies in low-density aggregations compared with at ambient P_{CO_2}. Despite mean calcification in the dark of densely aggregated corals declining by 45% at 1188 µatm P_{CO_2} compared with at ambient P_{CO_2}, increased calcification in the light under the same P_{CO_2} resulted in densely aggregated corals maintaining calcification rates over 24 h that were comparable to those maintained under ambient P_{CO_2}. However, light calcification rates were measured at peak light intensity (~700 µmol photons m^{-2} s^{-1}) and would be lower for a number of hours as the sun rises and sets over the course of a 12 h day, and it is unknown how corals would respond to treatment conditions under reduced light intensities. Both net and gross photosynthesis, as well as dark respiration, were unaffected by P_{CO_2} or colony density, suggesting that the changes in calcification rate attributed to colony density were not directly associated with photosynthesis or respiration. Nonetheless, the results demonstrate the value of considering neighbourhood effects created by closely spaced colonies when evaluating the impacts of elevated P_{CO_2} on coral populations. Neighbouring organisms, such as conspecifics, can modulate the physical environment experienced by coral colonies

on a reef, subsequently altering the physiological response of corals to elevated P_{CO_2}.

The implications of our calcification results are similar to those of recent studies in which it has been shown that macroalgae and seagrass beds can mitigate the negative effects of OA on calcifying organisms in both temperate and tropical coastal systems (Semesi et al., 2009; Cornwall et al., 2013). These effects accrue from the dense stands of macroalgae and seagrasses that create localized conditions of elevated seawater pH (compared with ambient conditions) beneath their canopies that promote biological calcification (Hurd, 2015). For example, on rocky reefs in New Zealand, canopies of the temperate macroalga *Carpophyllum maschalocarpum* can improve conditions in seawater for calcification by understorey crustose coralline algae (CCA) (Cornwall et al., 2015). Within such canopies, seawater flow is reduced compared with overlying bulk seawater flow, resulting in thickened DBLs around the CCA, and an increase in pH in the light (to 8.9) that favours calcification (Cornwall et al., 2015). In another study in New Zealand, canopies of the macroalga *Arthrocardia corymbosa* also benefitted calcification of understorey CCA by elevating pH within their canopies when the bulk flow of seawater had a reduced pH (7.65) (Cornwall et al., 2013). This effect was mediated through a combination of reduced water flow within the canopy and photosynthetic activity by the macroalga. Additionally, Chan et al. (2016) demonstrated for the corals *Favites* sp. and *Pocillopora damicornis* that exposure to reduced flow speeds enhanced their calcification when the overlying seawater was manipulated to a reduced pH (7.8) relative to ambient conditions (8.2). In these experiments, low flow speeds created thicker DBLs at the surface of the coral colonies, within which the metabolic activity of the coral tissue increased pH relative to bulk seawater pH (Chan et al., 2016).

Although it was beyond the scope of the present study to measure seawater chemistry (e.g. O_2 concentrations and pH in the DBL at the surface of the coral tissue) on a millimetre-to-centimetre scale between corals and among their branches, reduced flow speeds among colonies in the flume are a plausible mechanism underlying the reduced negative effects of elevated P_{CO_2} on calcification of corals in high-density aggregations. Together, reduced water flow and increased DBL thickness adjacent to the tissues of the densely aggregated colonies may have acted in concert with CO_2 uptake through photosynthesis by endosymbiotic *Symbiodinium* to elevate seawater pH in the DBL during the day (Chan et al., 2016). Although coral calcification reduces Ω_{arag} in seawater when the exchange of seawater is limited (Anthony et al., 2011), photosynthesis by *Symbiodinium* in the coral tissue can counteract these effects during the day, for example, as in *Acropora aspersa* incubated in large (550 litre) recirculating flumes maintained at 560–700 µatm P_{CO_2} (Anthony et al., 2013). Conversely, in the dark, aerobic respiration and calcification of *A. aspersa* depressed Ω_{arag} and hindered calcification, which represents conditions under which there was no potential for compensatory effects of photosynthesis by *Symbiodinium* to increase seawater pH (Anthony et al., 2013). Thus, while calcifying organisms can benefit from their metabolic activity, which locally elevates pH and Ω_{arag} of seawater in dense communities during the day, these conditions are reversed in the dark, and therefore have the potential to impede calcification.

The hypothesized concentration boundary layer created around the high-density aggregations employed in the present study is supported by visualization of the water flow among coral branches using brine shrimp eggs and plaster-of-Paris casts. The brine shrimp eggs revealed seawater being diverted over the first upstream corals

in the high-density aggregations (Fig. 3A), and subsequently over the entire length (i.e. 30 cm) of the aggregation. Seawater that passed among the colonies was contained longer among colonies in the high- versus the low-density aggregations, with these effects attributed to the formation of eddies between the colonies that retained seawater among branches (Fig. 3A). As a result, seawater typically was retained for ~2 s among colonies in the high-density aggregation, with some particles remaining in these locations as long as 3 s. Further, dissolution of plaster corals placed in high-density aggregates was reduced compared with the dissolution of plaster corals in low-density aggregates. These differences in dissolution of plaster corals suggest that the integrated flow speeds experienced by corals in the high-density aggregation were lower than those experienced in low-density aggregations. Reduced seawater flow within the dense aggregates has the potential to enhance net calcification under OA conditions by reducing the exposure of corals to low pH seawater, and thus reducing skeletal dissolution that would be expected to occur as seawater pH declines as a result of OA (Hurd, 2015; Chan et al., 2016).

Although calcification rates in the present study were affected by colony density and P_{CO_2}, photosynthesis and respiration were unaffected by the same conditions. The absence of an effect of colony density on photosynthesis and respiration suggests that the corals were not mass-transfer limited, at least for CO_2 and O_2, and within the range of flow speeds experienced by the colonies within the aggregates tested. Mass-transfer limitation is believed to be the main driver behind reduced metabolic rates for corals in low-flow conditions (Patterson et al., 1991; Lesser et al., 1994), where reduced seawater motion around a colony constrains the flux of metabolites, such as O_2, between the coral tissue and surrounding seawater (Helmuth et al., 1997; Reidenbach et al., 2006). The lack of an effect of P_{CO_2} on photosynthesis and respiration in the present study is consistent with the results of Comeau et al. (2016), who incubated nubbins (3–5 cm long) of P. verrucosa from the back reef of Moorea under a variety of P_{CO_2} regimes between 280 and 2000 µatm P_{CO_2}. Under similar conditions of light and temperature as employed herein (~700 µmol photons m^{-2} s^{-1} and 27°C), and using stirred incubation chambers, they found that rates of net photosynthesis and dark respiration were unaffected by P_{CO_2}. As a result, the consistent rates of net photosynthesis under elevated P_{CO_2} may have contributed to an increased pH in the DBL adjacent to the tissues of corals incubated at elevated P_{CO_2}, thereby increasing coral calcification (Chan et al., 2016). It is also possible, however, that our null result for the effect of P_{CO_2} on respiration and photosynthesis reflects elevated Type II error attributed to low sample sizes. Interpreting the implications of this possibility also depends on the effect size that is relevant to the hypothesis being tested, but assuming this is 30% of the mean control values, then power (1–β) was ~0.40 for net photosynthesis and respiration, and ~0.60 for gross photosynthesis. Although low, these values suggest that strong effects of P_{CO_2} would have been detected in the present study.

Overall, results from the present study make a compelling case for differential densities of branching coral colonies (i.e. aggregation types) mediating the sensitivity of coral communities in at least some habitats, for example, such as that created by the shallow reefs of Moorea. Extending the present results to natural communities will, however, require additional work to evaluate the effects of varying colony densities, differing colony sizes and more complex flow regimes. Notably, the high-density aggregations employed herein (i.e. 400 colonies m^{-2}) exceeded the density of conspecifics at 10 m depth on the outer reef of Moorea in 2014

(116 colonies m^{-2}), and do not include the full size of range of colonies for this species. Consideration of larger colonies (i.e. >4-cm diameter) in arrayed in differing densities could be important, because larger colonies are functionally unequal to smaller colonies in the way that they respond to P_{CO_2} (Edmunds and Burgess, 2016). Some of these effects are likely to be caused by self-shading for larger colonies, which would in turn influence photosynthesis, and could result in mass flux limitation for shaded colonies within aggregations. Finally, in situ flow regimes are more complex than was created in the flume, with wave action on shallow and exposed reefs, such as the outer reef of Moorea, typically results in oscillatory flow and potentially increased mixing within the branches of corals (Reidenbach et al., 2006). Thus, further manipulative studies using a variety of colony sizes and corals with different morphologies are required to test how the present neighbourhood effects extend to mixed coral communities under ecologically relevant flow regimes. Together with ecological modelling, manipulative long-term studies can build on the current research to assess how the responses recorded within the present coral aggregations relate to neighbourhood effects at the scale of entire coral reefs.

References
Anthony, K. R. N., Kleypas, J. A. and Gattuso, J.-P. (2011). Coral reefs modify their seawater carbon chemistry – implications for impacts of ocean acidification. Glob. Change Biol. **17**, 3655-3666.

Anthony, K. R. N., Diaz-Pulido, G., Verlinden, N., Tilbrook, B. and Andersson, A. J. (2013). Benthic buffers and boosters of ocean acidification on coral reefs. Biogeosciences **10**, 4897-4909.

Atkinson, M. J. and Bilger, R. W. (1992). Effects of water velocity on phosphate uptake in coral reef-hat communities. Limnol. Oceanogr. **37**, 273-279.

Bellwood, D. R. and Hughes, T. P. (2001). Regional-scale assembly rules and biodiversity of coral reefs. Science **292**, 1532-1535.

Bramanti, L. and Edmunds, P. J. (2016). Density-associated recruitment mediates coral population dynamics on a coral reef. Coral Reefs **35**, 543-553.

Brown, A. L. and Carpenter, R. C. (2015). Water flow influences the mechanisms and outcomes of interactions between massive Porites and coral reef algae. Mar. Biol. **162**, 459-468.

Bruno, J. F. and Bertness, M. D. (2001). Habitat modification and facilitation in benthic marine communities. In: Marine Community Ecology (ed. M. D. Bertness, S. D. Gaines and M. E. Hay), pp. 201-218. Sunderland, MA: Sinauer.

Bruno, J. F. and Edmunds, P. J. (1998). Metabolic consequences of phenotypic plasticity in the coral Madracis mirabilis (Duchassaing and Michelotti): the effect of

morphology and water flow on aggregate respiration. *J. Exp. Mar. Biol. Ecol.* **229**, 187-195.

Bruno, J. F., Stachowicz, J. J. and Bertness, M. D. (2003). Inclusion of facilitation into ecological theory. *Trends Ecol. Evol.* **18**, 119-125.

Buss, L. W. (1979). Bryozoan overgrowth interactions: the interdependence of competition for space and food. *Nature* **281**, 475-477.

Callaway, R. M. (2007). *Positive Interactions and Interdependence in Plant Communities*. Dordrecht, Netherlands: Springer.

Chadwick, N. E. and Morrow, K. M. (2011). Competition among sessile organisms on coral reefs. In *Coral reefs: An Ecosystem in Transition* (ed. Z. Dubinsky and N. Stambler), pp. 347-371. Dordrecht, Netherlands: Springer.

Chalker, B. E. and Taylor, D. L. (1978). Rhythmic variations in calcification and photosynthesis associated with the coral *Acropora cervicornis* (Lamarck). *Proc. R. Soc. Lond. B Biol. Sci.* **201**, 179-189.

Chan, N. C. S., Wangpraseurt, D., Kühl, M. and Connolly, S. R. (2016). Flow and coral morphology control coral surface pH: implications for the effects of ocean acidification. *Front. Mar. Sci.* **3**, 10.

Chisholm, J. R. M. and Gattuso, J.-P. (1991). Validation of the alkalinity anomaly technique for investigating calcification and photosynthesis in coral reef communities. *Limnol. Oceanogr.* **36**, 1232-1239.

Comeau, S., Carpenter, R. C. and Edmunds, P. J. (2016). Effects of pCO_2 on photosynthesis and respiration of tropical scleractinian corals and calcified algae. *ICES J. Mar. Sci.* fsv267. doi:10.1093/icesjms/fsv267.

Cornell, H. V. and Karlson, R. H. (2000). Coral species richness: ecological versus biogeographical influences. *Coral Reefs* **19**, 37-49.

Cornwall, C. E., Hepburn, C. D., Pilditch, C. A. and Hurd, C. L. (2013). Concentration boundary layers around complex assemblages of macroalgae: implications for the effects of ocean acidification on understory coralline algae. *Limnol. Oceanogr.* **58**, 121-130.

Cornwall, C. E., Pilditch, C. A., Hepburn, C. D. and Hurd, C. L. (2015). Canopy macroalgae influence understorey corallines' metabolic control of near-surface pH and oxygen concentration. *Mar. Ecol. Prog. Ser.* **525**, 81-95.

Dayton, P. K. (1971). Competition, disturbance, and community organization: the provision and subsequent utilization of space in a rocky intertidal community. *Ecol. Monogr.* **41**, 351-389.

Dennison, W. C. and Barnes, D. J. (1988). Effect of water motion on coral photosynthesis and calcification. *J. Exp. Mar. Biol. Ecol.* **115**, 67-77.

Denny, M. W. (1988). *Biology and Mechanics of the Wave Swept Environment*. Princeton, NJ: Princeton University Press.

Dickson, A. G., Sabine, C. L. and Christian, J. R. (2007). *Guide to Best Practices for Ocean CO_2 Measurements*, PICES Special Publication 3.

Edmunds, P. J. and Burgess, S. C. (2016). Size-dependent physiological responses of the branching coral *Pocillopora verrucosa* to elevated temperature and P_{CO2}. *J. Exp. Biol.* **219**, 3896-3906.

Edmunds, P. J., Leichter, J. J., Johnston, E. C., Tong, E. J. and Toonen, R. J. (2016). Ecological and genetic variation in reef-building corals on four Society Islands. *Limnol. Oceanogr.* **61**, 543-557.

Evensen, N. R. and Edmunds, P. J. (2016). Interactive effects of ocean acidification and neighboring corals on the growth of *Pocillopora verrucosa*. *Mar. Biol.* **163**, 148.

Evensen, N. R., Edmunds, P. J. and Sakai, K. (2015). Effects of pCO_2 on spatial competition between the corals *Montipora aequituberculata* and *Porites lutea*. *Mar. Ecol. Prog. Ser.* **541**, 123-134.

Finzi, A. C., van Breemen, N. and Canham, C. D. (1998). Canopy tree–soil interactions within temperate forests: species effects on soil carbon and nitrogen. *Ecol. Appl.* **8**, 440-446.

Harborne, A. R., Mumby, P. J., Kennedy, E. V. and Ferrari, R. (2011). Biotic and multi-scale abiotic controls of habitat quality: their effect on coral-reef fishes. *Mar. Ecol. Prog. Ser.* **437**, 201-214.

Helmuth, B. S. T., Sebens, K. P. and Daniel, T. L. (1997). Morphological variation in coral aggregations: branch spacing and mass flux to coral tissues. *J. Exp. Mar. Biol. Ecol.* **209**, 233-259.

Hench, J. L. and Rosman, J. H. (2013). Observations of spatial flow patterns at the coral colony scale on a shallow reef flat. *J. Geophys. Res. Oceans.* **118**, 1142-1156.

Henry, H. A. L. and Aarssen, L. W. (1999). The interpretation of stem diameter–height allometry in trees: biomechanical constraints, neighbour effects, or biased regressions? *Ecol. Lett.* **2**, 89-97.

Hurd, C. L. (2015). Slow-flow habitats as refugia for coastal calcifiers from ocean acidification. *J. Phycol.* **51**, 599-605.

Idjadi, J. A. and Edmunds, P. J. (2006). Scleractinian corals as facilitators for other invertebrates on a Caribbean reef. *Mar. Ecol. Prog. Ser.* **319**, 117-127.

Idjadi, J. A. and Karlson, R. H. (2007). Spatial arrangement of competitors influences coexistence of reef-building corals. *Ecology* **88**, 2449-2454.

Johnson, A. S. and Sebens, K. P. (1993). Consequences of a flattened morphology: effects of flow on feeding rates of the scleractimian coral *Meandrina meandrites*. *Mar. Ecol. Prog. Ser.* **99**, 99-114.

Jones, C. G., Lawton, J. H. and Shachak, M. (1997). Positive and negative effects of organisms as physical ecosystem engineers. *Ecology* **78**, 1946-1957.

Kayal, M., Lenihan, H. S., Pau, C., Penin, L. and Adjeroud, M. (2011). Associational refuges among corals mediate impacts of a crown-of-thorns starfish *Acanthaster planci* outbreak. *Coral Reefs* **30**, 827-837.

Lang, J. C. and Chornesky, E. A. (1990). Competition between scleractinian reef corals – a review of mechanisms and effects. *Ecosyst. World* **25**, 209-252.

Lesser, M. P., Weis, V. M., Patterson, M. R. and Jokiel, P. L. (1994). Effects of morphology and water motion on carbon delivery and productivity in the reef coral, *Pocillopora damicornis* (Linnaeus): diffusion barriers, inorganic carbon limitation, and biochemical plasticity. *J. Exp. Mar. Biol. Ecol.* **178**, 153-179.

Lewis, E. and Wallace, D. (1998). *Program Developed for CO_2 System Calculations. ORNL/CIAC-105*. Oak Ridge, TN: Oak Ridge National Laboratory, US Department of Energy.

McCulloch, M., Falter, J., Trotter, J. and Montagna, P. (2012). Coral resilience to ocean acidification and global warming through pH up-regulation. *Nat. Climate Change* **2**, 623-627.

Mehrbach, C., Culberson, C. H., Hawley, J. E. and Pytkowicx, R. M. (1973). Measurement of the apparent dissociation constants of carbonic acid in seawater at atmospheric pressure. *Limnol. Oceanogr.* **18**, 897-907.

Moss, R. H., Edmonds, J. A., Hibbard, K. A., Manning, M. R., Rose, S. K., Van Vuuren, D. P., Carter, T. R., Emori, S., Kainuma, M., Kram, T. et al. (2010). The next generation of scenarios for climate change research and assessment. *Nature* **436**, 747-756.

Moya, A., Tambutte, S., Tambutte, E., Zoccola, D., Caminiti, N. and Allemand, D. (2006). Study of calcification during a daily cycle of the coral *Stylophora pistillata*: implications for 'light-enhanced calcification'. *J. Exp. Biol.* **209**, 3413-3419.

Muscatine, L., Falkowski, P. G., Porter, J. W. and Dubinsky, Z. (1984). Fate of photosynthetic fixed carbon in light- and shade-adapted colonies of the symbiotic coral *Stylophora pistillata*. *Proc. R. Soc. Lond. B Biol. Sci.* **222**, 181-202.

Muschenheim, D. K., Grant, J. and Mills, E. L. (1986). Flumes for benthic ecologists: theory, construction and practice. *Mar. Ecol. Prog. Ser.* **28**, 185-196.

Patterson, M. R., Sebens, K. P. and Olson, R. R. (1991). In situ measurements of flow effects on primary production and dark respiration in reef corals. *Limnol. Oceanogr.* **36**, 936-948.

Quinn, G. P. and Keough, M. J. (2002). *Experimental Design and Data Analysis for Biologists*. Cambridge, UK: Cambridge University Press.

Reidenbach, M. A., Koseff, J. R., Monismith, S. G. and Steinbuckc, J. V. (2006). The effects of waves and morphology on mass transfer within branched reef corals. *Limnol. Oceanogr.* **51**, 1134-1141.

Roth, A. A., Clausen, C. D., Yahiku, P. Y., Clausen, V. E. and Cox, W. W. (1982). Some effects of light on coral growth. *Pacific Sci.* **36**, 65-81.

Sebens, K. P., Witting, J. and Helmuth, B. (1997). Effects of water flow and branch spacing on particle capture by the reef coral *Madracis mirabilis* (Duchassaing and Michelotti). *J. Exp. Mar. Biol. Ecol.* **211**, 1-28.

Semesi, I. S., Beer, S. and Björk, M. (2009). Seagrass photosynthesis controls rates of calcification and photosynthesis of calcareous macroalgae in a tropical seagrass meadow. *Mar. Ecol. Prog. Ser.* **382**, 41-47.

Stachowicz, J. J. (2001). Mutualism, facilitation, and the structure of ecological communities. *Bioscience* **51**, 235-246.

Stimson, J. and Kinzie, R. A. (1991). The temporal pattern and rate of release of zooxanthellae from the reef coral *Pocillopora damicornis* (Linnaeus) under nitrogen-enrichment and control conditions. *J. Exp. Mar. Biol. Ecol.* **153**, 63-74.

Thomas, F. I. M. and Atkinson, M. J. (1997). Ammonium uptake by coral reefs: effects of water velocity and surface roughness on mass transfer. *Limnol. Oceanogr.* **42**, 81-88.

Veron, J. E. N. (2000). *Corals of the World*, Vol. 1-3. Townsville, Australia: Australian Institute of Marine Science.

Vogel, S. and LaBarbera, M. (1978). Simple flow tanks for research and teaching. *Bioscience* **28**, 638-643.

Washburn, L. (2016). MCR LTER: Coral Reef: Ocean Currents and Biogeochemistry: salinity, temperature and current at CTD and ADCP mooring FOR01 from 2004 ongoing. Obtained from knb-lter-mcr.30.31.